ELSEVIER

European Journal of Radiology 60 (2006) 353–366

EJR
EUROPEAN JOURNAL OF RADIOLOGY

www.elsevier.com/locate/ejrad

Macromolecular MRI contrast agents for imaging tumor angiogenesis

Tristan Barrett, Hisataka Kobayashi, Martin Brechbiel, Peter L. Choyke *

Molecular Imaging Program and Radioimmune and Inorganic Chemistry Section, Radiation Oncology Branch, National Cancer Institute, Building 10, Room 1B40, Bethesda, MD 20892-1088, USA

Received 10 June 2006; received in revised form 11 June 2006; accepted 14 June 2006

Abstract

Angiogenesis has long been accepted as a vital process in the growth and metastasis of tumors. As a result it is the target of several novel anti-cancer medications. Consequently, there is an urgent clinical need to develop accurate, non-invasive imaging techniques to improve the characterization of tumor angiogenesis and the monitoring of the response to anti-angiogenic therapy. Macromolecular MR contrast media (MMCM) offer this diagnostic potential by preferentially exploiting the inherent hyperpermeable nature of new tumor vessels compared with normal vessels. Over the last 10–15 years many classes of MMCM have been developed. When evaluated with dynamic contrast enhanced (DCE) MRI, a number of MMCM have demonstrated *in vivo* imaging properties that correlate with *ex vivo* histological features of angiogenesis. The enhancement patterns with some MMCM have been reported to correlate with tumor grade, as well as show response to anti-angiogenic and anti-vascular drugs. Future applications of MMCM include targeted angiogenesis imaging and drug delivery of anti-cancer 'payloads'. Herein we discuss the best known MMCMs along with their advantages and disadvantages.

Keywords: Angiogenesis; MRI; Contrast media; Macromolecular contrast; Cancer; Dendrimers; Liposomes; Dextrans

1. Introduction

Angiogenesis is the process by which new blood vessels are formed. Physiologically, angiogenesis normally takes place during wound healing, embryogenesis, and corpus luteum formation. However, angiogenesis has also been known as an essential element of tumor growth and metastasis. Folkman is credited with the modern re-discovery of this process, and described the importance of angiogenesis to tumor growth in a landmark paper of 1971 [1]. When a tumor exceeds a diameter of 1–2 mm, diffusion from the surrounding vasculature alone is no longer sufficient to provide nutrients to a tumor's outer cells. Thus, if a tumor is to grow, new blood vessel growth, or neo-vascularization, is necessary. To this end, oncologists have focused on developing anti-angiogenic and anti-vascular drugs over the last 10–15 years. Anti-angiogenic agents target the tiny new blood vessel tufts generated during angiogenesis, whilst anti-vascular agents target the more mature and generally larger vessels which feed the angiogenic microvasculature. These agents have brought with them an increased need to monitor the microvasculature of tumors and, in turn, the efficacy of this drug therapy. Microvascular density (MVD) is one method, it is a measure of the average number of microvessels within a selected microscopic field. MVD has been shown to correlate with the frequency of tumor metastasis and decreased patient survival time in several cancers, including breast and prostate [2]. However, MVD has limitations; it does not demonstrate functionality within the vessels sampled, and it does not easily allow assessment of heterogeneity within the tumor, thus a particular sample may under- or over-estimate angiogenesis. MVD is also inherently invasive, and requires an intact tissue sample. Hence, there is a need to develop a reliable and non-invasive imaging technique for the *in vivo* monitoring of angiogenesis.

A normal vessel has an endothelial layer with tight junctions, surrounded by a tightly adherent basement membrane that is, in turn, surrounded by pericytes and smooth muscle cells to create a water-tight tube for the delivery of nutrients. Tumor vessels are hyperpermeable due to their disorganized angiogenic process, whereby their vessel walls are incompletely formed and are fragile. Tumor neo-vessels have large gaps between the endothelial cells and the basement membranes. Pericytes and smooth muscles are loosely adherent, allowing gaps in the integrity of the vessel wall [3]. The hyperpermeable nature of tumor vessels can be exploited by MR contrast

* Corresponding author. Tel.: +1 301 451 4220; fax: +1 301 402 3191.
E-mail address: pchoyke@nih.gov (P.L. Choyke).

0720-048X/$ – see front matter © 2006 Elsevier Ireland Ltd. All rights reserved.
doi:10.1016/j.ejrad.2006.06.025

agents. Agents that leak slowly through the normal vasculature are able to pass quickly through tumor vessels to produce differential enhancement. Traditional MR contrast agents such as gadolinium-diethylenetriamine pentaacetic acid (Gd-DTPA) have a low molecular weight (mW), <1000 Daltons (Da). Macromolecular contrast media (MMCM), also termed blood pool agents, were initially designed for prolonged intravascular retention and typically have mW > 30,000 Da [4]. The small size of Gd-DTPA allows it to diffuse quickly into the extracellular fluid space, even from relatively normal vessels, leading to large first-pass fractions. Normal, extra-cerebral microvessels are less permeable to molecules with increasing molecular weights, particularly so when the weight is >20 kDa and diameter >10 nm [6]. In contrast, even molecules with diameters as large as 400–600 nm are able to pass through the hyperpermeable vessels of tumors, albeit at a reduced rate [7]. Thus, low molecular weight agents (LMCM) extravasate non-selectively from the blood into the interstitium of both normal and tumor tissues, whereas MMCMs more selectively diffuse through and enhance angiogenic tissue. This is not entirely specific to cancer – severe inflammatory and reparative tissue has similar vasculature – but MMCMs are more specific for tumors than the LMCMs (Fig. 1).

One disadvantage of MMCMs is that the slower diffusion leads to a reduced concentration of Gd within tumor tissue, which may decrease apparent enhancement. This is partially compensated for by inherently higher relaxivity values due to the larger number of Gd atoms that are attached per molecule and slower rate of molecular rotation. The prolonged retention of MMCMs also provides a longer window to acquire images. The enhanced permeability and retention (EPR) effect may enable better MMCM-linked drug delivery to tumors; targeting permeable tumor tissue, whilst prolonged retention allows greater exposure to the drug and hence increased effectiveness.

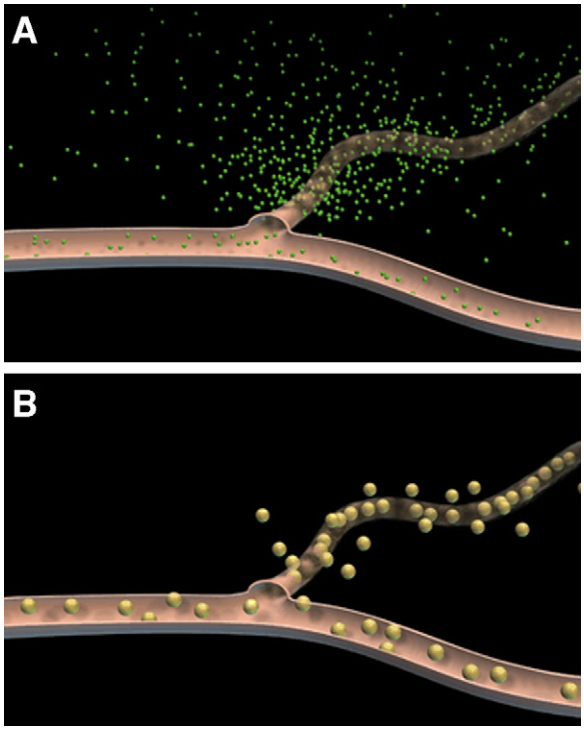

Fig. 1. Graphic representation of: (A) low molecular weight and (B) macromolecular contrast media diffusing from vasculature into the interstitial space.

A number of different MRI MMCMs have been developed over the last 20 years. Herein we discuss several of these, along with their advantages and disadvantages. MMCM suitable for CT imaging such as liposomes containing non-ionic iodinated contrast media or gold nanoparticles are not covered in this review as they are still at early stage of development and have not yet been adequately evaluated for imaging angiogenesis.

The ideal MMCM should have a long half-life to allow time for data collection, whilst having a good toxicity profile—a particular concern for compounds containing Gd [8]. It should also be able to selectively home in on pathological targets and have the potential for delivering adjunctive therapy. Other factors to be considered are the ease of production, uniformity in size, cost, and compatibility with scanning systems currently in use [8]. Some MMCM have the potential to act as drug delivery vectors for the selective targeting of chemotherapeutic medications or radio-sensitizers to tumor tissue. This would enable clinicians to maximize drug dose, whilst minimizing side-effects, and concurrently image the region of concern-so called 'image-based drug dosimetry'. We will explore these issues and postulate on future developments within the field.

2. The role of dynamic contrast-enhanced magnetic resonance imaging

Dynamic contrast-enhanced magnetic resonance imaging (DCE-MRI) is the acquisition of a consecutive series of MR images before, during, and after the administration of a contrast agent. CT can offer excellent resolution, combined with rapid scanning, and iodine measurements that are linearly related to signal. However, radiation exposure is a major limitation, particularly when multiple studies are required to follow lesions over time. Thus, DCE-MRI is generally preferable in this setting.

A complex description of DCE-MRI is beyond the scope of this article, but, essentially it relies on a kinetic model to derive estimates of tissue perfusion and permeability based on the shape of the tumor wash-in and wash-out curves. The results can be depicted numerically, or as color-encoded images. DCE-MRI parameters have been shown to correlate with vascular permeability, hence angiogenesis, within tumor tissue [9]. The parameter K^{trans} represents the rate of contrast agent transfer from blood to interstitium. It is dependant on blood flow and permeability. de Lussanet et al. showed that the size of the contrast agent affects this value; K^{trans} decreases as the molecular weight of the contrast agent increases [10]. This is because the rapid first-pass extraction of LMCMs means that blood flow predominantly determines K^{trans}, whereas, the slow diffusion of MMCMs means flow is less important and permeability becomes the major determining factor. Thus, MMCM K^{trans} values may more accurately reflect permeability and hence angiogenesis within tumors. The majority of DCE-MRI studies rely on LMCMs because of their clinical availability, but MMCMs are being increasingly investigated.

Early after the injection of contrast media, enhancement comes mainly from the blood vessels, and predominantly reflects blood volume and flow. Following this, the contrast medium quickly (within seconds) starts to leak into the interstitial space. MMCMs, due to their larger size, diffuse more slowly into the tumor interstitium than LMCMs. However, MMCMs are slower to wash out of the tumor and thus, the tumor-to-background contrast increases over time, whereas it quickly decreases with LMCMs due to their rapid wash-out [5]. As a result, imaging timing is not as critical with MMCMs.

In developing MMCMs for imaging of angiogenesis, the majority of studies have used the 'dynamic' imaging (*i.e.* rapidly acquired serial images), but some authors have relied on a limited number of 'static' MR images (*e.g.* at three time points), which provide snapshots of the enhanced tumor at fixed times after contrast injection. The choice of DCE-MRI or three time point methods is controversial and yet to be settled, however, regardless of the technique used, MMCMs yield very different data than LMCMs.

3. Types of macromolecular MRI contrast agents

3.1. Albumin-(gadolinium-DTPA) complexes

Albumin-(Gd-DTPA) is historically important as a macromolecular agent. It was first synthesized in 1987 by Ogan et al. [11]. In a typical synthesis of Gd labeled albumin, 25–35 molecules of Gd-DTPA are covalently bound to each albumin molecule, although it is possible to bind higher numbers. The complexes have an average molecular weight of approximately 92 kDa, with a diameter of ~6 nm. The volume of distribution is 0.05 L/kg, which closely approximates the body's relative blood volume. This is not surprising, given the nature of albumin as a vascular protein responsible for the maintenance of osmotic (water) pressure within blood vessels. As a result, the phrase "blood pool" agent was coined [7]. As such, albumin-(Gd-DTPA) has served as a prototype for macromolecular contrast media (MMCM).

In 1987, Schmeidl et al. characterized albumin-(Gd-DTPA) as an intravascular MRI contrast agent in animal models [12]. They used between nine and 18 Gd-DTPA chelates per albumin molecule, and showed significantly increased signal enhancement (*via* T1 effect) in liver, lung, myocardium, spleen, kidney, and brain tissue. The enhancement remained relatively constant for 30 min. Albumin-Gd complexes have been shown to be of use in MR angiography [13] and MR mammography [5,14]. Studies have shown albumin-(Gd-DTPA) is helpful in characterizing the microvessels of a wide range of tumors, including breast, sarcoma and prostate [5,15,16]. In the original formulations, albumin to Gd-DTPA bonds caused disruption of the chelate and allowed free Gd ion leakage and consequent toxicity. Subsequent authors have addressed this by improving the chelating agent (Fig. 2).

Marzola et al. have investigated the potential for DCE-MRI using albumin complexes as contrast agents. Initially they studied Gd-albumin's ability to demonstrate the anti-angiogenic effects of SU6668—an inhibitor of three separate receptor tyrosine kinases, including Flk-1/KDR for VEGF-2-receptor [17]. Early treatment efficacy was shown after 24 h of treatment, with a 51% (rim) and 26% (core) decrease in the average vessel permeability of the tumor. The same group compared albumin based macromolecular to LMCMs. The anti-angiogenic effect of SU11248 (an inhibitor of platelet-derived growth factor receptor tyrosine kinase) was assessed in mouse models containing human colon cancer xenografts [18]. Different analysis methods were used for each contrast agent to quantify the effect of treatment. The albumin complexed agent showed a 42% decrease in vascular permeability within the tumor rim, whilst DCE-MRI performed with Gd-DTPA alone showed a 31% decrease in the initial area under the concentration–time curve. Histology confirmed a significant difference in mean vessel density between treated and control groups. Daldrup et al. showed that results from albumin-(Gd-DTPA)-enhanced MRI correlated with histological breast tumor grade, which was not demonstrable with LMCMs [5]. Further studies have also supported the ability of albumin-(Gd-DTPA)-enhanced MRI to show early response of tumors to anti-angiogenic agents [19,20]. Studies have also correlated the albumin-(Gd-DTPA)-enhanced MRI measurement of permeability values (K^{trans}) with those of histological MVD following anti-angiogenic therapy [5,16,21].

A potential problem with albumin based macromolecular agents is the prolonged retention of Gd. Although the plasma half-life of the molecule is 3 h in rats, elimination is slow and incomplete and the compound has been shown to remain within the circulation for several weeks, particularly accumulating in the liver and bone [3]. This stems from the fact that only about

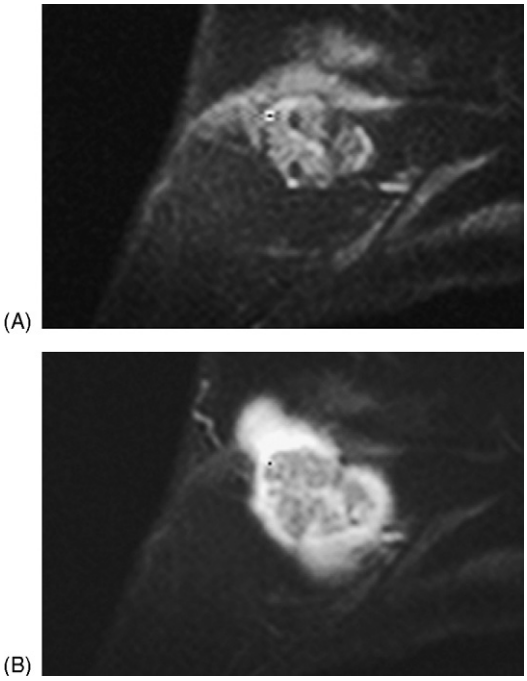

Fig. 2. CD1-nude ovariectomized mice, 34 days after rat ovary xenotransplantation. MMCM highlights angiogenic processes. (A) SE images obtained immediately after biotin-BSA-(Gd-DTPA) administration. (B) SE images acquired 40 min after biotin-BSA-(Gd-DTPA) administration. Reproduced with permission from M. Neeman and "Magnetic Resonance in Medicine". Ref.: Magn Reson Med 2004;52(October(4)):741–50.

5% of albumin leaks from the blood each hour—due, in part, to the molecule's propensity to form aggregates. Thus, any albumin complex will have prolonged retention in the intravascular space after intravascular injection [22].

Albumin is also potentially immunogenic and this may limit its development as an *in vivo* contrast agent and as a vector for targeted drug therapy [23]. The potential for immunogenicity, combined with its prolonged retention and risk of toxicity has stymied the early promise of albumin as a MMCM. Therefore, despite the favorable distribution profile of albumin-(Gd-DTPA), it has only been used in animal studies.

3.2. MS-325

In order to combat the problem of delayed Gd clearance associated with albumin-(Gd-DTPA) agents, Gd-chelates with reversible binding to albumin were developed. The theory behind these agents is that the reversible binding of albumin ensures that the low molecular weight Gd-chelate is released from the albumin and thus can be readily cleared from the body.

MS-325, an agent that reversibly binds to serum albumin, was first investigated as an MR contrast agent in 1996 by Lauffer et al. [24], was further characterized by Parmelee et al. [25] and has mainly been studied in MR angiography. This agent has been shown to bind strongly but reversibly to human serum albumin *in vitro*. MS-325 consists of a lipophilic chemical group (diphenylcyclohexyl) attached to a Gd-chelate by a phosphodiester linkage. The lipophilic group mediates protein binding, resulting in a reversible, non-covalent bond with albumin. MS-325 is injected in free form and subsequently binds to serum albumin *in vivo*. At high concentrations of the complex, as many as 30 molecules of MS-325 can bind to one albumin molecule. However, above a certain concentration any increase in the injected dose leads to an increase of the free form only, due to saturation of the albumin binding sites. The molecular weights of the 'free' MS-325 and of the albumin-bound forms are 957 and 68,000 Da, respectively, therefore only the bound form can be considered a macromolecular contrast agent. The equilibrium between free and bound MS-325 depends on the concentrations of the MS-325 and the plasma albumin (*i.e.* it is affected by low-albumin states), and on the albumin-binding affinity constant of the bound form [26] (Fig. 3).

The properties of MS-325 varies amongst species, therefore care needs to be taken in choosing animal models for study. In primates and rabbits, the elimination half-life is relatively long (2–3 h), whereas in rats it is shorter (25 min) [25]. This is mainly because rats exhibit lower protein binding of MS-325, particularly during the first 5 min after administration. The agent has a two-fold higher volume of distribution in rats compared to humans.

Corot et al. compared the relaxivity and concentration of MS-325, ultrasmall superparamagnetic iron oxide, and P792 (a macromolecular derivative of Gd-DOTA) in the bolus phase and steady-state phase in rabbits [27]. For MS-325, Gd blood concentration was measured over the first 5 min. Immediately after injection, 74% of MS-325 was in free form, however, at 1 min post-injection 75% of the MS-325 was bound to albumin. The

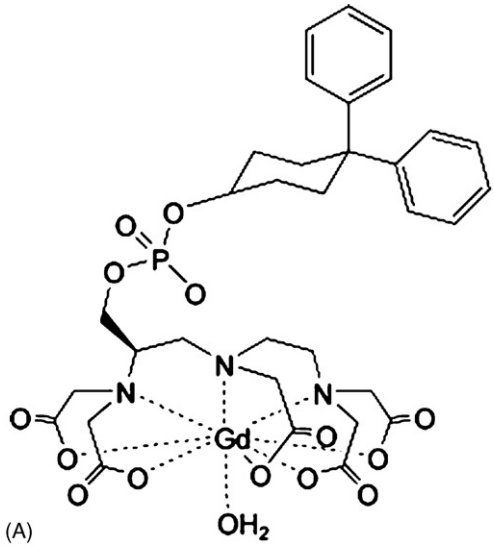

(A)

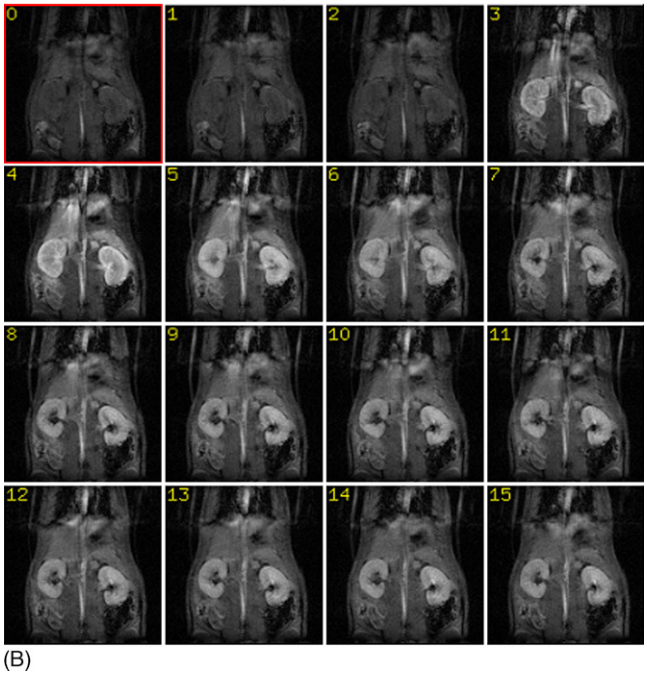

(B)

Fig. 3. (A) Schematic representation of MS-325. (B) MS-325 imaging in a rat model. Forty-minutes dynamic contrast-enhanced 4.7-T MRI using radio frequency spoiled gradient echo imaging sequence after injection of Gd-labeled MS325 (0.05 mmol/kg), first 16 repetitions shown. Image intensity changes in the kidneys indicated initial rapid contrast inflow through the renal arteries, accompanied by diffuse cortical enhancement, and followed by medullary enhancement which predominates in the later images. (A) Reproduced with permission from P. Caravan and "Chemistry". Ref.: Chem 2005;11(October(20)):5866–74.

extravasation of the free form of MS-325 during the bolus phase leads to tissue enhancement with kinetics similar to LMCMs, which may decrease the contrast between the vascular space and the adjacent tissue and would potentially be a disadvantage if used for tumor imaging.

Given the differences within animal models, it was essential to characterize the properties of MS-325 in human subjects. To this end, MS-325 was the first Gd-based macromolecular agent used in human trials [28]. In a Phase I study, seven volun-

teers received an intravenous injection of MS-325 at a dose of 0.05 mmol/kg over 30 s [29]. The authors reported no adverse reactions, and the dynamic MR angiography provided good vascular and selective arterial enhancement. Carotid MR angiography of patients in a Phase II study was completed without complications [30]. A Phase III study of MS-325 MR angiography in 174 patients with known or suspected peripheral vascular disease demonstrated no adverse events [31]. Patients received 0.03 mmol/kg MS-325 as a contrast agent for aorto-iliac MR angiography. Results were significantly better than MR without contrast and approached those obtained with conventional angiography.

There have been few studies on the use of MS-325 as a contrast agent in angiogenesis or tumor delineation. Turetschek et al. compared MS-325 to albumin-(Gd-DTPA) for imaging chemically induced breast tumors in rats [32]. MS-325 demonstrated no significant correlations to either MVD or tumor grade. Albumin-(Gd-DTPA) showed a significant correlation between K^{trans} and MVD, but fPV (a measure of plasma volume) values were not significantly different. As previously mentioned, problems may arise from the fact that a rodent model was used. Another obstacle is separation of the pharmacokinetics of the free and bound forms of MS-325. The imaging methods are sensitive to the paramagnetic effects produced by the Gd contained within both the free and bound forms of MS-325, although the latter would be expected to have greater relaxivity. Also the protein affinity of MS-325 in the interstitial space is unknown and may differ from that in plasma.

MS-325 has attractive advantages due to its toxicity profile, but has certain disadvantages when considered as a contrast agent for tumor imaging.

3.3. Dextran-(gadolinium-DTPA) complexes

Dextran is a linear polysaccharide consisting of a polymer of glucose molecules. Gd-DTPA moieties can be covalently attached to each dextran molecule *via* an easily hydrolysable bond. Dextran compounds have obvious advantages: they are inexpensive and have a well-established safety record in human subjects, having been used for over 50 years as a synthetic plasma expander [33]. Wang et al. first evaluated dextran-(Gd-DTPA) as a MMCM [34]. 15 Gd-DTPA chelates were complexed to each dextran molecule, resulting in a molecular weight of approximately 75 kDa. The contrast agent remained intravascular for at least 1 h after injection and showed enhancement of liver, spleen, kidneys, and myocardium. It is broken down more rapidly than albumin and has a shorter biological half-life, at 43 min. However, the distribution and subsequent elimination of dextrans is dependent on their molecular weight and charge [35]. Dextrans display a high degree of polydispersity, which makes estimates of permeability difficult, and leads to inconsistent results.

Dextran-(Gd-DTPA) has been mainly been investigated for MR angiography [36,37], acute myocardial infarction [38] and cardiac perfusion studies [39]. Sirlin et al. compared dextran-(Gd-DTPA) to a LMCM in rabbits with VX2 thigh tumors [40]. They conjugated an average of 187 gadolinium atoms per dextran, molecular weight 165 kDa, diameter 17.6 nm. This increased molecular size produced a prolonged intravascular half-life of approximately 58 h—calculated from imaging data of the vena cava, rather than serum measurements. The group demonstrated significantly greater enhancement of vena cava and aortic blood vessels at all time points. Within the tumor rim, contrast enhancement was higher in the control contrast group up until 1 h. This can be explained by the increased angiogenesis in this region, combined with the rapid leak of the LMCM across these hyperpermeable capillaries. Tumor rim enhancement with dextran-(Gd-DTPA) became equivalent to that of the LMCM at 1 h, was greater at 24 h and was seen up to 72 h post-injection. It should be noted that previous reports suggest an increased incidence of anaphylactic reactions with dextrans of higher molecular weights [35].There has been interest in the development of dextrans for drug delivery. They have a large number of hydroxyl groups that may be conjugated to drugs and proteins, either by direct attachment, or through a linker [41]. It is thought that dextrans are internalized by, and enter cells through fluid-phase endocytosis, a passive process [42]. In addition, dextrans are stable under mild acidic and basic conditions and are highly water soluble. Moreover, dextran complexes may also reduce the immunoreactivity of conjugated tumor-targeted monoclonal antibodies [43]. Dextrans have been used to modify the surface of liposomes and superparamagnetic iron oxide particles to produce MMCMs (*vide infra*).

3.4. Viral particles

Douglas et al. demonstrated the potential of the viral capsid of cowpea chlorotic mottle virus (CCMV), as a vector for either drug delivery or catalysis [44]. The virus' nucleic acids are removed, essentially leaving an empty 'protein cage'. The authors showed encapsulation of an anionic polymer *via* pH-dependent gating of the capsid's pores. CCMV was chosen because it can be purified in large quantities, is compatible with both hydrophobic and hydrophilic molecules, is less immunogenic, and its genes can be manipulated to introduce mutations at desired positions [45]. Coating with polyethylene glycol (PEG) reduces its immunogenicity and protects the virus from inducing a primary immune response [46].

In 2005, Allen et al. investigated the use of CCMV capsids complexed to Gd as an MR contrast agent [47]. CCMV-Gd was able to produce very high relaxivity values, thus showing that the compound has excellent potential as a MMCM. However, *in vivo* stability needs to be assessed; for instance, Ca^{2+} may compete for metal binding on the viral surface, destabilizing the complex. Immunogenicity also remains an issue, although plant viruses are less immunogenic than viruses that affect humans. There is potential to use the ability of viral capsids to transport encapsulated materials, or to use their mechanisms of cell entry to enable drug delivery.

3.5. Liposomes

Caride et al. was among the first to demonstrate the potential of liposomes to incorporate paramagnetic species and function as an MMCM for magnetic resonance imaging [48]. Liposomes

are spherical vesicles 20–400 nm in diameter. These consist of one or more bilayer phospholipid membranes (or lamella) and a hydrophilic interior. It is possible to incorporate paramagnetic material into the membrane or the aqueous inner chamber of liposomes. The biggest disadvantage of liposomes is their polydispersity, making reproducible synthesis difficult.

Unger et al. showed significant improvement in MR contrast between liver and tumor with Liposome-(Gd-DTPA) vesicles in rats with hepatic metastases [49]. They tested 70 and 400 nm diameter vesicles. The smaller liposomes produced the greatest enhancement per unit weight, reflecting their larger surface-area-to-volume ratio. Liposome-(Gd-DTPA) also resulted in sustained vascular enhancement for 1 h after administration. Further liposome studies have incorporated other paramagnetic species such as $MnCl_2$ [50] and iron oxide [51] (Fe_3O_4)-also termed 'ferrosomes' or 'magnetoliposomes' (*vide infra*).

The selective imaging of the liver, and also spleen, is due to the preferential uptake of liposomes by macrophages within the reticulo-endothelial system (RES) cells in the spleen and liver (Kupffer cells). Thus, liposomes were initially developed as liver imaging contrast agents. In order to delay blood clearance and target other organs, researchers have coated liposomes with PEG [52]. The ability of these vesicles to avoid uptake by the RES has lead to the term 'stealth' liposome [53]. PEG coating also serves to increase vesicle recirculation and may help in 'passive' targeting of tumors [52]. A study comparing PEG-coated and dextran-coated (Gd-DTPA)-liposomes [54] showed superior accumulation of dextran agents in the lymph nodes, but a 3–3.5-fold increase in lymph node signal intensity within the PEG group. This may be explained by increased relaxivity of PEG-modified Gd-liposomes (Fig. 4).

Some groups have investigated the targeting of liposome contrast agents to tumors. The endothelial integrin $\alpha_V\beta_3$ is known to be expressed on angiogenic vessels, and has been shown to correlate with tumor grade [55]. Sipkins et al. targeted a liposomal contrast agent to this receptor *via* the monoclonal antibody LM609 and showed increased tumor enhancement in rabbits [56]. Mulder et al. produced liposomes with ~700 $\alpha_V\beta_3$-specific RGD peptides attached [57]. The liposomes contained Gd and fluorescein-PE for MR and fluorescence imaging, respectively. *In vivo* T1 MR images showed enhancement and *ex vivo* fluorescent microscopy demonstrated the association of the liposomes with activated tumor epithelium.

Niosomes are constructed from non-ionic surfactant vesicles instead of phospholipids. Niosomes have the advantage of being more stable *in vitro* than traditional liposomes. They have been investigated as targeted contrast agents. Luciani et al. successfully targeted PEG-coated niosomes bearing glucose conjugates to prostate carcinoma xenografts in mice [58]. They showed that adding PEG moieties up to 2000 Da mW increased tumor accumulation of the MMCM without diminishing signal intensity.

Liposomes have long been investigated as vectors for delivering drugs. This application pre-dates their development as imaging agents [59]. Most recent work has centered on targeting liposomes by conjugating them to antibodies [60], although other targeting candidates include peptides [61], folates, aptamers, and polysaccarides [62]. Antibodies by themselves increase the hydrodynamic diameter of the conjugate whereas the smaller agents do not significantly enlarge the outer diameter of the construct. The future of targeted liposomes is uncertain given the difficulties with synthesis reproducibility. However, liposomes with less tissue specificity are more desirable, because they could be taken up by a wider variety of tumor types.

3.6. Dendrimers

Dendrimers are a class of highly branched synthetically produced spherical polymers. Their exterior can be functionalized with primary amine groups, which allow attachment of a large numbers of Gd-chelates to their surface. Dendrimers have a well defined structure and can be produced to a specific physical size with consistency and reproducibility. This eliminates polydispersity issues that are associated with other MMCMs. Two types are commercially available: polyamidoamine (PAMAM), first developed in 1990 [63], and diaminobutane core polypropylimine (DAB or PPI) [64]. Dendrimers were first used as MR contrast agents by Wiener et al. in 1994 [65]. DAB dendrimers have a pure aliphatic polyamine core in contrast to the PAMAM dendrimers that have an amide functional group core component [66]. Both types of dendrimer can be synthesized to different 'generations', which increase in size and molecular weight in proportion to their generation (*e.g.* Generation 4 dendrimers are half the size of Generation 8 dendrimers when functionalized with chelated Gd) (Fig. 5).

Another class of dendrimer-based MR contrast agents is the Gadomers developed by Schering AG. These are spherical molecules that possess similar properties to those of dendrimers. Their internal structure incorporates aromatic rings, they are simpler and more compact and thus smaller in size as compared to the PAMAM or DAB dendrimer-based agents of the same generation [67]. Gadomer-17 is the largest in the series and approximates the size of G3 dendrimers. This agent has a rapid renal elimination and has shown promise as a MMCM, particularly in the field of MR lymphangiography [68] and myocardial perfusion imaging [69].

The variation in size of the dendrimer generations leads to different pharmacokinetics and pharmacodynamics and, therefore, different imaging properties. Changing dendrimer size, up to 15 nm in diameter, has been shown to alter their permeability across the vascular wall, excretion route, and their recognition by the RES [70]. The spherical nature of dendrimers means that the molecular size, *i.e.* diameter, is directly proportional to their molecular weight, with only minimal conformational change possible.

Dendrimer based contrast agents of less than 5 nm diameter (*i.e.* G2 or G3) leak rapidly from the vasculature into surrounding tissue, although not as quickly as Gd-DTPA [71]. Dendrimer based contrast agents of 3–6 nm diameter (*i.e.* G2, G3, G4) are quickly excreted *via* the kidney, primarily during the first pass—as such they may prove useful in renal imaging [72]. Molecules between 5 and 8 nm (G4, G5) are able to selectively leak through hyperpermeable tumor vessels. Dendrimer based contrast agents larger than 8 nm diameter (G6 and above) demonstrate good vascular enhancement, but only minimal leak-

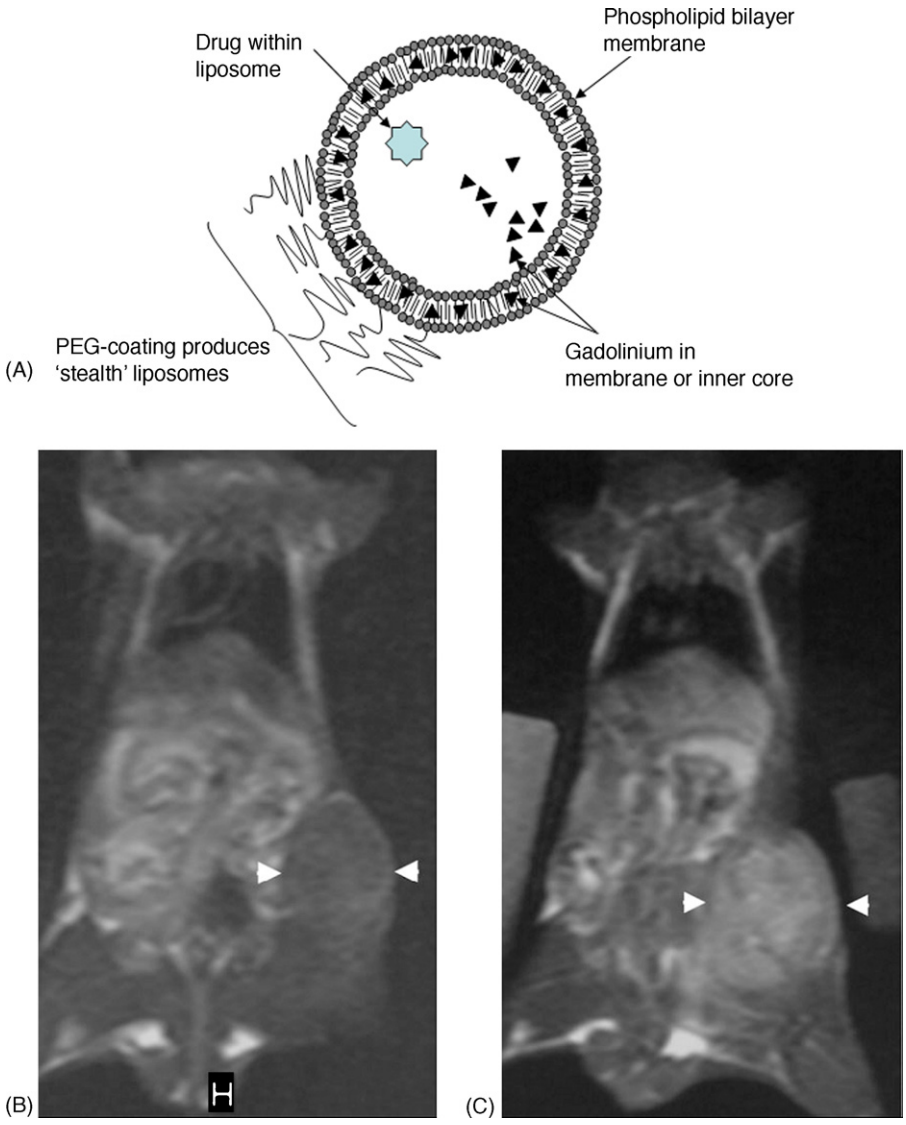

Fig. 4. (A) Schematic representation of liposome structure. T1-weighted images of a mouse (B) before and (C) 20 h after the injection of PEG-stabilized paramagnetic liposomes. (B and C) Reproduced with permission from I. Bertini and "Magnetic Resonance in Medicine". Ref.: Magn Reson Med 2004;52(September(3)):669–72.

Table 1
Comparison of the different dendrimer generations

Macromolecular PAMAM dendrimer based MRI contrast agents [69]				
Generation	# primary amines available for Gd-DTPA conjugation	Molecular weight (kDa)	Diameter (nm)	Excretion route
G2	16	15	3	Kidney
G3	32	29	5	Kidney
G4	64	59	6	Kidney
G5	128	88	7	Mostly kidney
G6A	192	175	8	Liver and kidney
G6E	256	238	9	Mostly liver
G7	512	470	11	Liver
G8	1024	954	13	Liver
G9	2048	1910	14	Liver
G10	4096	3820	15	Liver

Gd: Gadolinium, DTPA: diethylenetriamine pentaacetic acid, kDa: kilo-Daltons, nm: nanometers. G6A = containing ammonia core, G6E = containing ethylenediamine core.

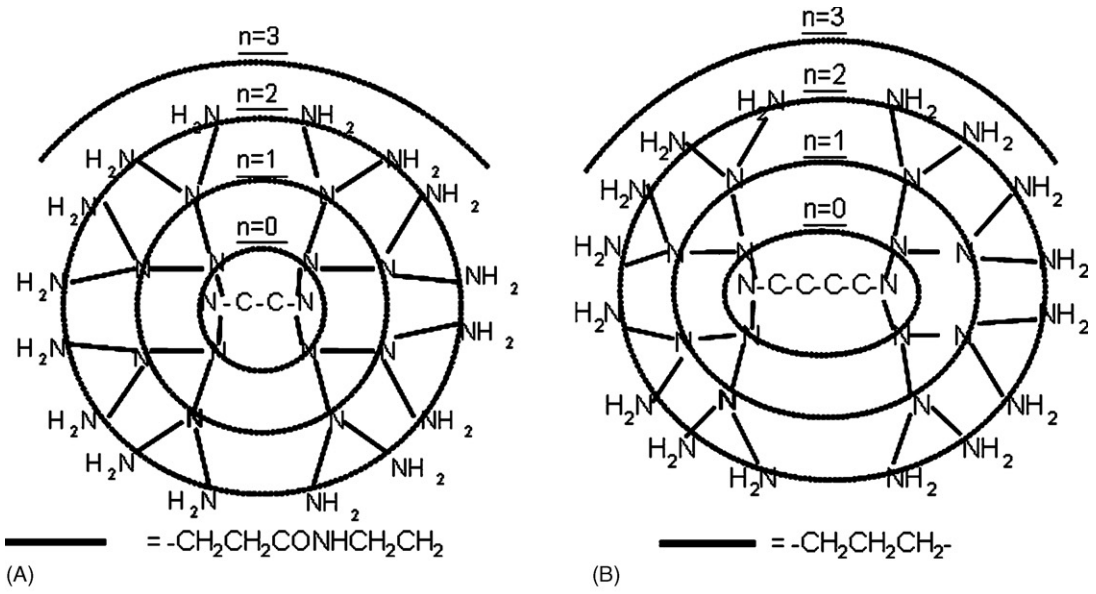

Fig. 5. (A) Schematic representation of PAMAM dendrimer. (B) Schematic representation of DAB dendrimer (n = generation). (C) G6 dendrimer MRA depicting the vascular of a mouse with a mammary xenograft implanted on the upper back (TUBO mammary tumor).

age from tumor vessels into surrounding tumor tissue [66]. G9 and G10 dendrimer based contrast agents are taken up by the RES within the liver and spleen. Altering the hydrophilic or hydrophobic nature of the dendrimers also affects their pharmacokinetics. Increasing the hydrophilicity of G4 dendrimers by PEG-ylation was shown to reduce renal excretion and liver accumulation, hence prolonging half-life and enhancing blood vessel visualization [73]. The DAB core dendrimers are more

hydrophobic than PAMAM and, as such, have been shown to accumulate in the liver and may prove advantageous in hepatic imaging [74]. Larger hydrophilic agents are useful for lymph imaging. DAB-G5 has been used to identify individual lymph nodes and PAMAM-G4 to visualize the lymphatic system [75] (Table 1).

Yordanov et al. used dynamic dendrimer-enhanced MRI to image tumors in mouse models [76]. PAMAM-Gd-G8 (13 nm) enhanced the tumor vasculature, whereas the analogous, smaller G6 (10 nm) agent, showed better delineation of the tumor tissue. Kobayashi et al. investigated the use of avidin chase techniques to control the contrast signal from a PAMAM-G6 dendrimer [77]. Within 2 min of the addition of avidin-biotin, the contrast agent was trapped in the liver, clearing the blood pool of enhancement. This system may allow multiple injections of a contrast agent during an MR session and enable better visualization of permeability, hence angiogenesis, within tumors. However, avidin is very immunogenic, thus it will be unsuitable for human use unless similar, less immunogenic alternatives are found. Kobayashi et al. used a PAMAM-G8 dendrimer to show the early effects of radiation therapy on tumor vessel permeability [78]. Thus, it is possible to monitor the effects of this and/or concurrent therapies and establish when the vessels are suitably permeable to allow targeted drug treatment.

Dendrimers, because of their multiple potential binding sites, have excellent potential for drug delivery and as targeted imaging agents. Kojima et al. demonstrated the ability of PEGylated PAMAM dendrimers to act as vectors for the anti-cancer drugs adriamycin and methotrexate [79]. Quintana et al. used a PAMAM-G5 dendrimer containing methotrexate to target a human epidermoid cancer cell line through a folic acid receptor [80]. Targeted delivery was demonstrated and the cytotoxic effect of methotrexate was increased 100-fold compared to the free drug alone. Sukla et al. have demonstrated the ability of dendrimers to target angiogenic vessels [81]. They synthesized a PAMAM-G5 dendrimer conjugated to a RGD-4C ligand. This ligand targets the angiogenic marker $\alpha_V\beta_3$ integrin. Flow cytometry demonstrated the uptake of this complex by human umbilical vein endothelial cells expressing $\alpha_V\beta_3$ receptors. Other examples of targeting include that of prostate specific membrane antigen (over-expressed in some prostate cancers) by a monoclonal-antibody linked to PAMAM-G5 dendrimer [82].

Vincent et al. used a dendrimer-oligomer vector to target cancer cells for gene therapy [83]. They delivered angiostatin and metalloprotease inhibitor (TIMP-2) genes to mouse models of breast cancer. Tumor-associated vascularization was greatly reduced and the combined delivery of the two genes resulted in a 96% inhibition of tumor growth.

The work of Backer et al. shows the potential of dendrimers to deliver radionuclide sensitizing agents [84]. They used a PAMAM-G5 dendrimer linked to boron atoms. The molecule was then conjugated to the thiol groups of VEGF to allow tumor cell targeting. Accumulation in mouse breast cancer cells was demonstrated with a Cy5 marker and near infrared imaging. Uptake was more apparent at the tumor periphery, where angiogenesis is greatest. This bioconjugate has the potential to enable targeted 'boron neutron capture therapy' of the tumor neo-vasculature.

3.7. Iron oxides

Iron oxides are inherently paramagnetic and produce their effects predominantly by shortening T2 relaxation time. This causes a 'negative' enhancement, *i.e.* tissue uptake produces a less intense signal. Iron oxide agents have the added advantage of having a well recognized pathway for break-down and excretion, unlike gadolinium. Degradation causes iron to enter the plasma, where it is processed by the body. Risk of iron overload is minimal; an average dose of contrast agent is comparable to iron contained in less than one unit of blood [85].

Super-paramagnetic iron oxide (SPIO) particles were first studied as MR contrast agents in humans in 1988 [86]. SPIOs consist of a poly-crystalline magnetite core coated with either dextran (ferumoxides) or silicon (ferumoxsils), producing particles with a diameter of 50–150 nm. The physiologic distribution of iron oxide particles depends on the size of particles and the physiochemical property of their coating. Following intravenous administration, dextran-coated SPIOs are taken up by phagocytic cells within the RES (approximately 82.6% go to the liver and 6.2 ± 7.6% to the spleen) [87]. Tumors tend to contain fewer phagocytic cells, thus appear brighter than surrounding tissue, which takes up the contrast agent. Stark et al. were able to significantly increase the number of detected hepatic lesions and reduce the size threshold for detection of lesions to 3 mm [88]. Doses of up to 50 μmol/kg of iron were used, subsequent experiments have used lower doses and a slow infusion rate to avoid side-effects, notably hypotension. These results, however, have been superceded by advances in MR imaging that render normal liver darker, thus increasing the contrast with imbedded tumors. The SPIO agents AMI-25 (ferumoxide) and SHU 555 have been clinically approved for the detection of liver metastases. Monocrystalline iron oxide nanocompounds (MION) have also been developed. In contrast to SPIOs, they consist of a monocrystalline core. Their hexagonal shaped electron-dense cores have approximately 25 dextran molecules attached, resulting in a hydrodynamic radius of 20 nm [89] (Fig. 6).

Ultrasmall super-paramagnetic iron oxides (USPIO) are less than 50 nm in diameter—thus, as their name implies, they are smaller than SPIOs. Weissleder et al. first developed USPIOs by fractionation of AMI-25, to produce particles of less than 10 nm diameter [90]. These smaller particles were able to avoid uptake by the RES, resulting in a half-life of 81 min (compared to 6 min for AMI-25). This property means they are better suited as 'blood pool' agents. USPIO also have additional effects on T1 relaxation and have been shown to accumulate in bone marrow and lymph nodes. Examples include AMI-227 (Combidex).

USPIOs have great potential in the field of lymph node imaging. Weissleder et al. first showed that metastatic lymph nodes take up iron oxide particles to a lesser extent than normal (benign) nodes and thus do not change in signal intensity, *i.e.* appear brighter than normal nodes [91]. This is because metastatic tumors replace normal lymph node tissue or produce changes in lymphatic flow, hence reducing their accumulation

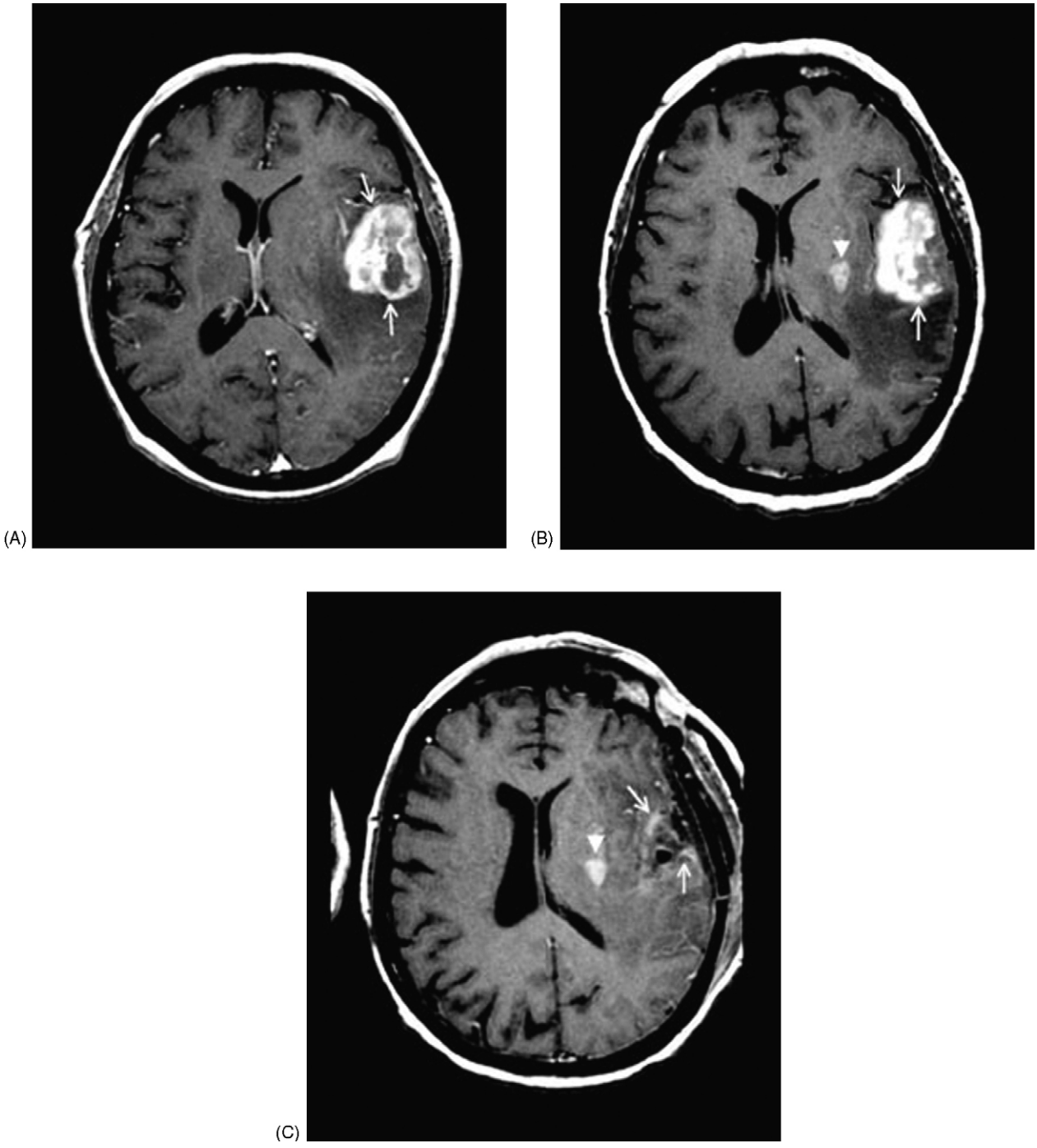

Fig. 6. Imaging with dextran-coated iron oxide nanoparticles. (A) Gadolinium-enhanced SE T1-weighted image shows a large left fronto-parietal enhancing tumor (arrows). (B) At 24 h after ferumoxtran infusion, SE T1-weighted image demonstrates tumor enhancement (arrows). Additionally, a new enhancing lesion showed up medially, in the putamen (arrowhead). Surgery was performed after this scan. (C) At 5 days after ferumoxtran infusion and 4 days after surgery, postoperative SE T1-weighted image reveals still clear visualization of the residual ferumoxtran-enhancing lesion in the putamen (arrowhead). Histochemistry for iron showed uptake in reactive cells (astrocytes and macrophages) rather than tumor cells. The persistence of the MMCM in tumor cells at 2–5 days confers advantages for post operative imaging assessment. Reproduced with permission from E. Neuwelt and "Neuropathology and Applied Neurobiology". Ref.: Neuropathol Appl Neurobiol 2004;30(October(5)):456–71.

of macrophage-containing USPIO particles. Baghi et al. showed that USPIO contrast agents detected metastatic lymph nodes in head and neck cancers with a sensitivity of 82.3% and specificity of 100% [92]. Head, neck, and pelvic lymph nodes are easier to image due to reduced respiratory or cardiac motion artifact. The intravenous use of USPIO enables imaging of the entire body's lymph nodes. This is a significant improvement over traditional lymphangiographic methods, whereby only lymph nodes in the drainage pathway of the interstitial injection can be imaged.

USPIOs also have potential for the imaging of angiogenesis. Turetschek et al. showed the ability of the USPIO NC100150 to demonstrate angiogenesis in murine models of breast cancer [16]. There was a significant correlation between the dynamic permeability values obtained and histology (as indicated by MVD). Despite being a considerably larger molecule, the USPIO produced similar results when compared to albumin-(Gd-DTPA). In a similar trial design, USPIO-dynamic MRI derived permeability values have been shown to correlate with histologically defined tumor grade [93]. Turetschek et al. went on to show the ability of USPIOs to monitor anti-angiogenic drug therapy [21]. Athymic rats implanted with a human breast cancer cell line were treated with a VEGF receptor tyrosine kinase inhibitor. USPIO permeability values correlated with MVD and demonstrated treatment efficacy. de Lussanet et al. compared NC100150 to the weak albumin binding agent Gd-BOPT (gadobenate dimeglumine) in mice with colon carcinoma xenografts [94]. Both agents produced similar results and correlated with histological MVD. Kostourou et al. also demonstrated the ability of USPIOs to show early neo-vascularization of gliomas, whilst highlighting the role of tumor-induced nitric oxide inhibitors in this process [95].

More recently very small superparamagnetic iron oxide particles (VSOP) have been developed [96]. VSOPs are coated with monomers as opposed to polymers. The monomer of choice is citrate, for example, VSOP-C63 and C184. The overall particle diameter of VSOP can be varied between 2 and 10 nm. VSOPs show promise in the field of MR angiography [97] and, in particular, coronary angiography [98].

There are limited examples of iron oxide compounds being used to target cancer cells. Artemov et al. demonstrated the *in vitro* ability of SPIOs, conjugated to Herceptin mAbs, to target HER-2/neu receptors on the surface of malignant breast cancer cells [99]. However, the complexes formed by conjugating SPIO to mAbs are large and are unlikely to avoid uptake by the RES *in vivo*, thus preventing delivery to the target site. The smaller particles, MION, have been successfully targeted to intracranial carcinoma xenografts [100].

The potential for iron oxide compounds to provide therapeutic drug or gene delivery is increased *via* incorporation into liposomes (magnetoliposomes). Bulte et al. have investigated the use of magnetoliopsomes [51]. Uptake of this contrast agent was particularly apparent in bone marrow. PEG-ylation of the magnetoliposomes selectively enhanced their T2 relaxivity by 10–15%.

A recent development is the use of superparamagnetic iron species to label stem cells. Within the field of cancer research this method may allow endothelial targeting to areas of neovascularization and enable delivery of gene therapy to certain cancers. SPIO particles can be incorporated into endosomes within the stem cell cytoplasm. The iron particles are not toxic to the cell and do not affect their ability to function or differentiate [101]. Typically incorporation is *via* transfection agents, alternative approaches include monoclonal antibody complexes or magnetodendrimers [102]. The iron particles allow *in vivo* tracking of the cells by MR imaging. Anderson et al. demonstrated the ability to monitor Sca1 + stem cells in a glioma model [103]. After intravenous injection these endothelial precursor cells migrate towards angiogenic stimuli and are incorporated into the tumor neovasculature. The cells can continue to be imaged during their life span. This group showed that tumors demonstrated uptake of the stem cells, with 'enhanced', hypo-

Table 2
Comparison of macromolecular contrast media (MMCM)

MMCM	Para-magnetic agent	Size	Tested for humans?	MR applications	Comments
Albumin-(Gd-DTPA)30	Gd	92 kDa	No	Tumor angiogenesis, Angiography, Mammography	Experimental only. Also used in anti-angiogenesis drug research
MS-325	Gd	68 kDa	Yes	Angiography, Lymphangiography	
Dextran-(Gd-DTPA)15	Gd	75 kDa	Yes	Angiography, Cardiac perfusion studies	High polydispersity. Also used to coat liposomes and iron oxide MMCMs
Dextran-(Gd-DTPA)187	Gd	165 kDa	Yes		
Liposomes	Gd or Iron	20–400 nm	No	Liver and spleen imaging, Lymhangiography	High polydispersity. Good potential for drug delivery
Viral particles: CCMV	Gd	28 nm	No	Angiogenesis	Developmental stages only
Dendrimers	Gd	15 kDa (G2), 88 kDa (G5), 3820 kDa (G10)	No	Lymphangiography, Tumor vasculature (larger generations)	Potential for targeting imaging and drug delivery
SPIO	Iron	50–150 nm	Yes	Liver metastases	Negative contrast agents. Ferumoxides licensed for liver imaging
USPIO	Iron	10–50 nm	Yes	Lymphangiography, Tumor angiogenesis	Potential for drug delivery, targeted imaging and stem cell imaging
VSOP	Iron	2–10 nm	No	Angiography	

Gd: Gadolinium, kDa: kilo-Daltons, nm: nanometers, CCMV: cowpea chlorotic mottle virus, SPIO: superparamagnetic iron oxide, USPIO: ultrasmall superparamagnetic iron oxide, VSOP: very small superparamagnetic iron oxide.

dense regions. Histology confirmed the presence of iron-labeled endothelial-like (*i.e.* differentiated) cells around the tumor rim, where angiogenesis is maximal. This technique demonstrates the potential for stem cell imaging of angiogenesis and the ability to monitor its progression over time (Table 2).

4. Summary

Angiogenesis is an important process in the growth and metastasis of tumors. The development of anti-angiogenic drugs has further increased the need to develop accurate imaging techniques. MMCM are able to exploit the hyperpermeable vessels produced by tumor angiogenesis to selectively enhance lesions. MMCM are either inherently paramagnetic, or incorporate paramagnetic transition metals, such as gadolinium or manganese. Several MMCMs have been developed and tested in clinical trials, some have the ability to demonstrate angiogenesis, whereas others are better for angiography or lymphangiography imaging. Iron oxide species and dendrimers are the most studied MMCMs and appear to offer the best potential for imaging angiogenesis. The prototype agent, albumin-(Gd-DTPA), is still utilized as a research tool.

The future of MMCM imaging is exciting. There is the possibility of developing 'smart' (activated) agents, which respond to, and enhance following, a particular *in vivo* stimulus. Examples include pH or pO_2 levels, which differ from normal to tumor tissue. MMCMs will be major players in the field of molecular imaging, with the further development of targeted agents. Tumor cell targeting can be *via* monoclonal antibodies, aptamers or peptides. An important target epitope is likely to be the integrin $\alpha_V\beta_3$, which is a marker of angiogenesis. Liposomes, dendrimers and viral particles are the most likely candidates as vectors to deliver therapeutic agents directly to tumor cells.

MMCMs have a key role to play in the imaging of angiogenesis and, potentially, the delivery of anti-cancer therapy. Unfortunately, the rate at which these agents are being approved for clinical use is worryingly slow. The reasons for this impediment need to be addressed before their immense potential of MMCMs can be tapped.

Acknowledgements

This research was supported by the Intramural Research Program of the NIH, National Cancer Institute, Center for Cancer Research. Thank you to Michal Neeman, Edward Neuwelt, Ivano Bertini and Peter Caravan for permission to use their images.

References

[1] Folkman J. Tumor angiogenesis: therapeutic implications. N Engl J Med 1971;285:1182–6.
[2] Weidner N, Semple JP, Welch WR, Folkman J. Tumor angiogenesis and metastasis—correlation in invasive breast carcinoma. N Engl J Med 1991;324:1–8.
[3] Benjamin LE, Golijanin D, Itin A, Pode D, Keshet E. Selective ablation of immature blood vessels in established human tumors follows vascular endothelial growth factor withdrawal. J Clin Invest 1999;103:159–65.
[4] Padhani AR. MRI for assessing antivascular cancer treatments. Br J Radiol 2003;76:S60–80.
[5] Daldrup H, Shames D, Wendland M, et al. Correlation of dynamic contrast-enhanced magnetic resonance imaging with histologic tumor grade: comparison of macromolecular and small molecular contrast media. Am J Roentgenol 1998;171:941–9.
[6] Desser T, Rubin D, Muller H, et al. Dynamics of tumor imaging with Gd-DTPA-polyethylene glycol polymers: dependence on molecular weight. J Magn Reson Imaging 1994;4:467–72.
[7] Daldrup-Link HE, Brasch RC. Macromolecular contrast agents for MR mammography: current status. Eur Radiol 2003;13:354–65.
[8] Wickline SA, Lanza GM. Molecular imaging, targeted therapeutics, and nanoscience. J Cell Biochem Suppl 2002;39:90–7.
[9] Padhani AR, Husband JE. Dynamic contrast-enhanced MRI studies in oncology with an emphasis on quantification, validation and human studies. Clin Radiol 2001;56:607–20.
[10] de Lussanet QG, Langereis S, Beets-Tan RG, et al. Dynamic contrast-enhanced MR imaging kinetic parameters and molecular weight of dendritic contrast agents in tumor angiogenesis in mice. Radiology 2005;235:65–72.
[11] Ogan MD, Schmiedl U, Moseley ME, Grodd W, Paajanen H, Brasch RC. Albumin labeled with Gd-DTPA. An intravascular contrast-enhancing agent for magnetic resonance blood pool imaging: preparation and characterization. Invest Radiol 1987;22:665–71.
[12] Schmiedl U, Ogan M, Paajanen H, et al. Albumin labeled with Gd-DTPA as an intravascular, blood pool-enhancing agent for MR imaging: biodistribution and imaging studies. Radiology 1987;162:205–10.
[13] Wolf CL, Moseley ME, Wikstrom MG, et al. Assessment of myocardial salvage after ischemia and reperfusion using magnetic resonance imaging and spectroscopy. Circulation 1989;80:969–82.
[14] Brasch R, Shames D, Cohen F, et al. Quantification of capillary permeability to macromolecular magnetic resonance imaging contrast media in experimental mammary adenocarcinomas. Invest Radiol 1994;2(Suppl.):8–11.
[15] Gossmann A, Okuhata Y, Shames DM, et al. Prostate cancer tumor grade differentiation with dynamic contrast-enhanced MR imaging in the rat: comparison of macromolecular and small-molecular contrast media—preliminary experience. Radiology 1999;213:265–72.
[16] Turetschek K, Huber S, Floyd E, et al. MR imaging characterization of microvessels in experimental breast tumors by using a particulate contrast agent with histopathologic correlation. Radiology 2001;218:562–9.
[17] Marzola P, Degrassi A, Calderan L, et al. Early antiangiogenic activity of SU11248 evaluated *in vivo* by dynamic contrast-enhanced magnetic resonance imaging in an Experimental Model of Colon Carcinoma. Clin Cancer Res 2005;11:5827–32.
[18] Marzola P, Degrassi A, Calderan L, et al. *In vivo* assessment of antiangiogenic activity of SU6668 in an Experimental Colon Carcinoma Model. Clin Cancer Res 2004;10:739–50.
[19] Daldrup-Link HE, Okuhata Y, Wolfe A, et al. Decrease in tumor apparent permeability-surface area product to a MRI macromolecular contrast medium following angiogenesis inhibition with correlations to cytotoxic drug accumulation. Microcirculation 2004;11:387–96.
[20] Turetschek K, Preda A, Floyd E, et al. MRI monitoring of tumor response following angiogenesis inhibition in an experimental human breast cancer model. Eur J Nucl Med Mol Imaging 2003;30:448–55.
[21] van Dijke CF, Brasch RC, Roberts TP, et al. Mammary carcinoma model: correlation of macromolecular contrast-enhanced MR imaging characterizations of tumor microvasculature and histologic capillary density. Radiology 1996;198:813–8.
[22] Zhang Z, Nair SA, McMurry TJ. Gadolinium meets medicinal chemistry: MRI contrast agent development. Curr Med Chem 2005;12:751–78.
[23] Baxter AB, Lazarus SC, Brasch RC. *In vitro* histamine release induced by magnetic resonance imaging and iodinated contrast media. Invest Radiol 1993;28:308–12.
[24] Lauffer RB, Parmelee DJ, Ouellet HS, et al. MS-325: a small-molecule vascular imaging agent for magnetic resonance imaging. Acad Radiol 1996;3:S356–8.

[25] Parmelee D, Walovitsch C, Ouellet H, et al. Preclinical evaluation of the pharmacokinetics, biodistribution and elimination of MS-325, a blood pool agent for magnetic resonance imaging. Invest Radiol 1997;32: 741–7.
[26] Cavagna FM, Maggioni F, Castelli PM, et al. Gadolinium chelates with weak binding to serum proteins. Invest Radiol 1997;32:780–96.
[27] Corot C, Violas X, Robert P, Gagneur G, Port M. Comparison of different types of blood pool agents (P792, MS325, USPIO) in a rabbit MR angiography-like protocol. Invest Radiol 2003;38:311–9.
[28] Zhang Y, Choyke PL, Lu H, et al. Detection and localization of proteinuria by dynamic contrast-enhanced magnetic resonance imaging using MS325. J Am Soc Nephrol 2005;16:1727–52.
[29] Grist TM, Korosec FR, Peters DC, et al. Steady-state and dynamic MR angiography with MS-325: initial experience in humans. Radiology 1998;207:539–44.
[30] Bluemke DA, Stillman AE, Bis KG, et al. Carotid MR angiography: phase II study of safety and efficacy for MS-325. Radiology 2001;219: 114–22.
[31] Goyen M, Edelman M, Perreault P, et al. MR angiography of aortoiliac occlusive disease: a phase III study of the safety and effectiveness of the blood-pool contrast agent MS-325. Radiology 2005;236:825–33.
[32] Turetschek K, Floyd E, Helbich T, et al. MRI assessment of microvascular characteristics in experimental breast tumors using a new blood pool contrast agent (MS-325) with correlations to histopathology. J Magn Reson Imaging 2001;14:237–42.
[33] de Belder D. Medical application of dextran and its derivatives. In: Dumitriu S, editor. Polysaccharides in medicinal applications. New York: Marcel Dekker; 1996. p. 505–24.
[34] Wang SC, Wikstrom MG, White DL, et al. Evaluation of Gd-DTPA-labeled dextran as an intravascular MR contrast agent: imaging characteristics in normal rat tissues. Radiology 1990;175:483–8.
[35] Mehvar R. Dextrans for targeted and sustained delivery of therapeutic and imaging agents. J Control Rel 2000;69:1–25.
[36] Kroft LJ, Doornbos J, Benderbous S, de Roos A. Equilibrium phase MR angiography of the aortic arch and abdominal vasculature with the blood pool contrast agent CMD-A2-Gd-DOTA in pigs. J Magn Reson Imaging 1999;9:777–85.
[37] Loubeyre P, Canet E, Zhao S, Benderbous S, Amiel M, Revel D. Carboxymethyl-dextran-gadolinium-DTPA as a blood-pool contrast agent for magnetic resonance angiography. Experimental study in rabbits. Invest Radiol 1996;31:288–93.
[38] Wikstrom M, Martinussen HJ, Wikstrom G, et al. MR imaging of acute myocardial infarction in pigs using Gd-DTPA-labeled dextran. Acta Radiol 1992;33:301–8.
[39] Casali C, Janier M, Canet E, et al. Evaluation of Gd-DOTA-labeled dextran polymer as an intravascular MR contrast agent for myocardial perfusion. Acad Radiol 1998;5(Suppl. 1):S214–8.
[40] Sirlin CB, Vera DR, Corbeil JA, et al. Gadolinium-DTPA-dextran: a macromolecular MR blood pool contrast agent. Acad Radiol 2004;11:1361–9.
[41] Schacht E. Polysaccharide macromolecules as drug carriers. In: Illum L, Davis SS, editors. Polymers in controlled drug delivery. Bristol: Wright; 1987. p. 131–51.
[42] Lake J, Licko V, Van Dyke R, Scharschmidt B. Biliary secretion of fluid-phase markers by the isolated perfused rat liver. Role of transcellular vesicular transport. J Clin Invest 1985;76:676–84.
[43] Fagnani R, Halpern S, Hagan M. Altered pharmacokinetic and tumor localization properties of Fab' fragments of a murine monoclonal anti-CEA antibody by covalent modification with low molecular weight dextran. Nucl Med Commun 1995;16:362–9.
[44] Douglas T, Young M. Host–guest encapsulation of materials by assembled virus protein cages. Nature 1998;393:152–5.
[45] Wang Q, Lin T, Tang L, Johnson J, Finn M. Icosahedral virus particles as addressable nanoscale building blocks. Angew Chem Int Ed 2002;41:459–62.
[46] Raja KS, Wang Q, Gonzalez MJ, Manchester M, Johnson JE, Finn MG. Hybrid virus-polymer materials. 1. Synthesis and properties of PEG-decorated cowpea mosaic virus. Biomacromolecules 2003;4:472–6.
[47] Allen M, Bulte JW, Liepold L, et al. Paramagnetic viral nanoparticles as potential high-relaxivity magnetic resonance contrast agents. Magn Reson Med 2005;54:807–12.
[48] Caride VJ, Sostman HD, Winchell RJ, Gore JC. Relaxation enhancement using liposomes carrying paramagnetic species. Magn Reson Imaging 1984;2:107–12.
[49] Unger EC, Winokur T, MacDougall P, et al. Hepatic metastases: liposomal Gd-DTPA-enhanced MR imaging. Radiology 1989;171:81–5.
[50] Niesman MR, Bacic GG, Wright SM, Swartz HJ, Magin RL. Liposome encapsulated $MnCl_2$ as a liver specific contrast agent for magnetic resonance imaging. Invest Radiol 1990;25:545–51.
[51] Bulte JW, de Cuyper M, Despres D, Frank JA. Short- vs. long-circulating magnetoliposomes as bone marrow-seeking MR contrast agents. J Magn Reson Imaging 1999;9:329–35.
[52] Papahadjopoulos D, Allen TM, Gabizon A, et al. Sterically stabilized liposomes: improvements in pharmakokinetics and antitumor therapeutic efficacy. Proc Natl Acad Sci USA 1991;88:11460–4.
[53] Maruyama K, Kennel SJ, Huang L. Lipid composition is important for highly efficient target binding and retention of immunoliposomes. Proc Natl Acad Sci USA 1990;87:5744–8.
[54] Trubetskoy V, Cannillo J, Milshtein A, Wolf G, Torchilin V. Controlled delivery of Gd-containing liposomes to lymph nodes: surface modification may enhance MRI contrast properties. Magn Reson Imaging 1995;13:31–7.
[55] Brooks PC, Clark RA, Cheresh DA. Requirement of vascular integrin alpha Vbeta 3 for angiogenesis. Science 1994;264:569–71.
[56] Sipkins D, Cheresh D, Kazemi M, Nevin L, Bednarski M, Li K. Detection of tumor angiogenesis *in vivo* by alphaVbeta3-targeted magnetic resonance imaging. Nat Med 1998;4:623–6.
[57] Mulder WJ, Strijkers GJ, Habets JW, et al. MR molecular imaging and fluorescence microscopy for identification of activated tumor endothelium using a bimodal lipidic nanoparticle. FASEB J 2005;14:2008–10.
[58] Luciani A, Olivier JC, Clement O, et al. Glucose-receptor MR imaging of tumors: study in mice with PEGylated paramagnetic niosomes. Radiology 2004;231:135–42.
[59] Schwendener RA. The preparation of large volumes of homogeneous, sterile liposomes containing various lipophilic cytostatic drugs by the use of a capillary dialyzer. Cancer Drug Deliv 1986;3:123–9.
[60] Koning GA, Kamps JA, Scherphof GL. Efficient intracellular delivery of 5-fluorodeoxyuridine into colon cancer cells by targeted immunoliposomes. Cancer Detect Prev 2002;26:299–307.
[61] Pastorino F, Brignole C, Marimpietri D, et al. Vascular damage and anti-angiogenic effects of tumor vessel-targeted liposomal chemotherapy. Cancer Res 2003;63:7400–9.
[62] Matsukawa S, Yamamoto M, Ichinose K, et al. Selective uptake by cancer cells of liposomes coated with polysaccharides bearing 1-aminolactose. Anticancer Res 2000;20:2339–44.
[63] Tomalia D, Naylor A, Goddard III W. Starburst dendrimers: molecular-level control of size, shape, surface chemistry, topology, and flexibility from atoms to macroscopic matter. Angew Chem Int Ed Engl 1990;29:138–75.
[64] Malik N, Wiwattanapatapee R, Klopsch R, et al. Dendrimers: relationship between structure and biocompatibility *in vitro*, and preliminary studies on the biodistribution of 125I-labelled polyamidoamine dendrimers *in vivo*. J Control Rel 2000;65:133–48.
[65] Wiener E, Brechbiel M, Brothers H, et al. Dendrimer-based metal chelates: a new class of magnetic resonance imaging contrast agents. Magn Reson Med 1994.
[66] Kobayashi H, Brechbiel M. Dendrimer-based nanosized MRI contrast agents. Curr Pharm Biotechnol 2004;5:539–49.
[67] Misselwitz B, Schmitt-Willich H, Ebert W, Frenzel T, Weinmann H. Pharmacokinetics of Gadomer-17, a new dendritic magnetic resonance contrast agent. MAGMA 2001;12:128–34.
[68] Misselwitz B, Schmitt-Willich H, Michaelis M, Oellinger J. Interstitial magnetic resonance lymphography using a polymeric t1 contrast agent: initial experience with Gadomer-17. Invest Radiol 2002;37:146–51.
[69] Gerber B, Bluemke D, Chin B, et al. Single-vessel coronary artery stenosis: myocardial perfusion imaging with Gadomer-17 first-pass MR imag-

ing in a swine model of comparison with gadopentetate dimeglumine. Radiology 2002;225:104–12.
[70] Kobayashi H, Brechbiel M. Nano-sized MRI contrast agents with dendrimer cores. Adv Drug Deliv Rev 2005;57:2271–86 [Epub 2005 Nov 10. Review].
[71] Dong Q, Hurst D, Weinmann H, Chenevert T, Londy F, Prince M. Magnetic resonance angiography with gadomer-17. An animal study original investigation. Invest Radiol 1998;33:699–708.
[72] Sato N, Kobayashi H, Hiraga A, et al. Pharmacokinetics and enhancement patterns of macromolecular MR contrast agents with various sizes of polyamidoamine dendrimer cores. Magn Reson Med 2001;46:1169–73.
[73] Kobayashi H, Kawamoto S, Saga T, et al. Positive effects of polyethylene glycol conjugation to generation-4 polyamidoamine dendrimers as macromolecular MR contrast agents. Magn Reson Med 2001;46:781–8.
[74] Kobayashi H, Kawamoto S, Saga T, et al. Novel liver macromolecular MR contrast agent with a polypropylenimine diaminobutyl dendrimer core: comparison to the vascular MR contrast agent with the polyamidoamine dendrimer core. Magn Reson Med 2001;46:795–802.
[75] Kobayashi H, Kawamoto S, Choyke PL, et al. Comparison of dendrimer-based macromolecular contrast agents for dynamic micro-magnetic resonance lymphangiography. Magn Reson Med 2003;50:758–66.
[76] Yordanov A, Kobayashi H, English S, et al. Gadolinium-labeled dendrimers as biometric nanoprobes to detect vascular permeability. J Mater Chem 2003;13:1523–5.
[77] Kobayashi H, Kawamoto S, Star R, Waldmann T, Brechbiel M, Choyke P. Activated clearance of a biotinylated macromolecular MRI contrast agent from the blood pool using an avidin chase. Bioconjugate Chem 2003;14:1044–7.
[78] Kobayashi H, Reijnders K, English S. Application of a macromolecular contrast agent for detection of alterations of tumor vessel permeability induced by radiation. Clin Cancer Res 2004;15(10):7712–20.
[79] Kojima C, Kono K, Maruyama K, Takagishi T. Synthesis of polyamidoamine dendrimers having poly(ethylene glycol) grafts and their ability to encapsulate anticancer drugs. Bioconjugate Chem 2000;11:910–7.
[80] Quintana A, Raczka E, Piehler L, et al. Design and function of a dendrimer-based therapeutic nanodevice targeted to tumor cells through the folate receptor. Pharm Res 2002;19:1310–6.
[81] Shukla R, Thomas T, Peters J, Kotlyar A, Myc A, Baker Jr J. Tumor angiogenic vasculature targeting with PAMAM dendrimer-RGD conjugates. Chem Commun (Camb) 2005;14:5739–41.
[82] Patri A, Myc A, Beals J, Thomas T, Bander N, Baker Jr J. Synthesis and *in vitro* testing of J591 antibody-dendrimer conjugates for targeted prostate cancer therapy. Bioconjug Chem 2004;15:1174–81.
[83] Vincent L, Varet J, Pille JY, et al. Efficacy of dendrimer-mediated angiostatin and TIMP-2 gene delivery on inhibition of tumor growth and angiogenesis: *in vitro* and *in vivo* studies. Int J Cancer 2003;105:419–29.
[84] Backer M, Gaynutdinov T, Patel V, et al. Vascular endothelial growth factor selectively targets boronated dendrimers to tumor vasculature. Mol Cancer Ther 2005;4:1423–9.
[85] Anzai Y. Superparamagnetic iron oxide nanoparticles: nodal metastases and beyond. Top Magn Reson Imaging 2004;15:103–11.
[86] Weissleder R, Hahn P, Stark D, et al. Superparamagnetic iron oxide: clinical application as a contrast agent for MR imaging of the liver. Radiology 1988;168:297–301.
[87] Weissleder R, Stark D, Engelstad B, et al. Superparamagnetic iron oxide: pharmacokinetics and toxicity. AJR Am J Roentgenol 1989;152:167–73.
[88] Stark D, Weissleder R, Elizondo G, et al. Superparamagnetic iron oxide: clinical application as a contrast agent for MR imaging of the liver. Radiology 1988;168:297–301.
[89] Shen T, Weissleder R, Papisov M, Bogdanov Jr A, Brady T. Monocrystalline iron oxide nanocompounds (MION): physicochemical properties. Magn Reson Med 1993;29:599–604.
[90] Weissleder R, Elizondo G, Wittenberg J, Rabito C, Bengele H, Josephson L. Ultrasmall superparamagnetic iron oxide: characterization of a new class of contrast agents for MR imaging. Radiology 1990;175:489–93.
[91] Weissleder R, Guillermo E, Wittenberg J, et al. Ultrasmall superparamagnetic iron oxide: an intravenous contrast agent for assessing lymph nodes with MRI. Radiology 1990;175:494–8.
[92] Baghi M, Mack M, Hambek M, et al. The efficacy of MRI with ultrasmall superparamagnetic iron oxide particles (USPIO) in head and neck cancers. Anticancer Res 2005;25:3665–70.
[93] Turetschek K, Roberts T, Floyd E, et al. Tumor microvascular characterization using ultrasmall superparamagnetic iron oxide particles (USPIO) in an experimental breast cancer model. J Magn Reson Imaging 2001;13:882–8.
[94] de Lussanet Q, Backes W, Griffioen A, van Engelshoven J, Beets-Tan R. Gadopentetate dimeglumine versus ultrasmall superparamagnetic iron oxide for dynamic contrast-enhanced MR imaging of tumor angiogenesis in human colon carcinoma in mice. Radiology 2003;229:429–38.
[95] Kostourou V, Robinson SP, Whitley G, Griffiths J. Effects of overexpression of dimethylarginine dimethylaminohydrolase on tumor angiogenesis assessed by susceptibility magnetic resonance imaging. Cancer Res 2003;63:4960–6.
[96] Pilgrimm H. Superparamagnetische teilchen mit vergrösserter T1-relaxivität, verfahren zur herstellung und deren veerwendung. German patent PCT/DE 97/00578; 1997.
[97] Taupitz M, Schnorr J, Abramjuk C, et al. New generation of monomer-stabilized very small superparamagnetic iron oxide particles (VSOP) as contrast medium for MR angiography: preclinical results in rats and rabbits. J Magn Reson Imaging 2000;12:905–11.
[98] Taupitz M, Schnorr J, Wagner S, et al. Coronary MR angiography: experimental results with a monomer-stabilized blood pool contrast medium. Radiology 2002;222:120–6.
[99] Artemov D, Mori N, Okollie B, Bhujwalla Z. MR molecular imaging of the Her-2/neu receptor in breast cancer cells using targeted iron oxide nanoparticles. Magn Reson Med 2003;49:403–8.
[100] Remsen L, McCormick C, Roman-Goldstein S, et al. MR of carcinoma-specific monoclonal antibody conjugated to monocrystalline iron oxide nanoparticles: the potential for noninvasive diagnosis. Am J Neuroradiol 1996;17:411–8.
[101] Arbab A, Bashaw L, Miller B, Jordan E, Bulte J, Frank J. Intracytoplasmic tagging of cells with ferumoxides and transfection agent for cellular magnetic resonance imaging after cell transplantation: methods and techniques. Transplantation 2003;76:1123–30.
[102] Frank J, Zywicke H, Jordan E, et al. Magnetic intracellular labeling of mammalian cells by combining (FDA-approved) superparamagnetic iron oxide MR contrast agents and commonly used transfection agents. Acad Radiol 2002;9:S484–8.
[103] Anderson S, Glod J, Arbab A, et al. Noninvasive MR imaging of magnetically labeled stem cells to directly identify neovasculature in a glioma model. Blood 2005;105:420–5.